Single-particle tracking uncovers dynamics of glutamate-induced retrograde transport of NF-κB p65 in living neurons

Widera, D., Klenke, C., Nair, D., Heidbreder, M., Malkusch, S., Sibarita, J.-B., Choquet, D., Kaltschmidt, B., Heilemann, M. and Kaltschmidt, C. (2016) Single-particle tracking uncovers dynamics of glutamate-induced retrograde transport of NF-κB p65 in living neurons. Neurophotonics, 3 (4). 041804. ISSN 2329-4248 doi: https://doi.org/10.1117/1.NPh.3.4.041804 Available at https://centaur.reading.ac.uk/63751/

Neurophotonics

Neurophotonics.SPIEDigitalLibrary.org

Single-particle tracking uncovers dynamics of glutamate-induced retrograde transport of NF-κB p65 in living neurons

Darius Widera
Christin Klenke
Deepak Nair
Meike Heidbreder
Sebastian Malkusch
Jean-Baptiste Sibarita
Daniel Choquet
Barbara Kaltschmidt
Mike Heilemann
Christian Kaltschmidt

SPIE.

Darius Widera, Christin Klenke, Deepak Nair, Meike Heidbreder, Sebastian Malkusch, Jean-Baptiste Sibarita, Daniel Choquet, Barbara Kaltschmidt, Mike Heilemann, Christian Kaltschmidt, "Single-particle tracking uncovers dynamics of glutamate-induced retrograde transport of NF-κB p65 in living neurons," *Neurophoton.* **3**(4), 041804 (2016), doi: 10.1117/1.NPh.3.4.041804.

Neurophotonics 3(4), 041804 (Oct–Dec 2016)

Single-particle tracking uncovers dynamics of glutamate-induced retrograde transport of NF-κB p65 in living neurons

Darius Widera,[a,b,*,†] Christin Klenke,[a,†] Deepak Nair,[c,d] Meike Heidbreder,[e,‡] Sebastian Malkusch,[f] Jean-Baptiste Sibarita,[c,d,g] Daniel Choquet,[c,d] Barbara Kaltschmidt,[a,h] Mike Heilemann,[f,*] and Christian Kaltschmidt[a,*]

[a]University of Bielefeld, Cell Biology, Universitätsstr. 25, 33501 Bielefeld, Germany
[b]University of Reading, School of Pharmacy, Stem Cell Biology and Regenerative Medicine, Whiteknights, Reading RG6 6UB, United Kingdom
[c]University of Bordeaux, Interdisciplinary Institute for Neuroscience, 146 rue Léo-Saignat, Bordeaux 33077, France
[d]CNRS UMR 5297, 146 rue Léo-Saignat, Bordeaux 33077, France
[e]Julius-Maximilians-Universität, Department of Biotechnology and Biophysics, Am Hubland, Würzburg 97074, Germany
[f]Johann Wolfgang Goethe-University, Institute for Physical and Theoretical Chemistry, Max-von-Laue-Street 7, Frankfurt 60438, Germany
[g]Bordeaux Imaging Center, UMS 3420 CNRS, US4 INSERM, France
[h]University of Bielefeld, Molecular Neurobiology, Universitätsstr. 25, Bielefeld 33501, Germany

Abstract. Retrograde transport of NF-κB from the synapse to the nucleus in neurons is mediated by the dynein/dynactin motor complex and can be triggered by synaptic activation. The caliber of axons is highly variable ranging down to 100 nm, aggravating the investigation of transport processes in neurites of living neurons using conventional light microscopy. We quantified for the first time the transport of the NF-κB subunit p65 using high-density single-particle tracking in combination with photoactivatable fluorescent proteins in living mouse hippocampal neurons. We detected an increase of the mean diffusion coefficient (D_{mean}) in neurites from 0.12 ± 0.05 to 0.61 ± 0.03 $\mu m^2/s$ after stimulation with glutamate. We further observed that the relative amount of retrogradely transported p65 molecules is increased after stimulation. Glutamate treatment resulted in an increase of the mean retrograde velocity from 10.9 ± 1.9 to 15 ± 4.9 $\mu m/s$, whereas a velocity increase from 9 ± 1.3 to 14 ± 3 $\mu m/s$ was observed for anterogradely transported p65. This study demonstrates for the first time that glutamate stimulation leads to an increased mobility of single NF-κB p65 molecules in neurites of living hippocampal neurons. [DOI: 10.1117/1.NPh.3.4.041804]

Keywords: retrograde transport; single-particle tracking with photoactivated-localization microscopy; single molecule; NF-kappaB; neurons.

Paper 15050SSRR received Oct. 30, 2015; accepted for publication Apr. 18, 2016; published online May 18, 2016.

1 Introduction

The inducible transcription factor NF-κB is involved in crucial brain functions including learning and memory formation.[1–7] The most abundant NF-κB heterodimer detected within the central nervous system is composed of p65 and p50.[3,8,9] We and others have shown that NF-κB is localized in the synapse, can be activated by glutamate at synaptic sites, and is transported back to the nucleus after its activation.[3,10–15]

Axons and dendrites represent specialized neuronal cytoplasmic extensions, where movement by random diffusion alone would not permit efficient and directed delivery of proteins over long distances.[16,17] However, signals generated at synapses must be transported back to the nucleus to regulate gene expression (reviewed in Ref. 17).

Anterograde (away from nucleus) and retrograde (toward the nucleus) transports are crucial for the physiological function of neurons and are mediated by motor proteins including dynein and kinesins.[18,19] Due to their polarized nature and the relatively long distance between the nucleus and the periphery, neurons are highly dependent on intact active transport machinery (reviewed in Ref. 20). Consequently, defects in axonal transport are involved in the development of several neurodegenerative diseases, including Alzheimer's, Parkinson's, and Huntington's disease.[21] We and others have previously demonstrated that neuronal NF-κB is actively transported toward the nucleus by the minus end-directed motor protein dynein (Refs. 11, 22, 23; Fig. 1). In contrast, diffusion seems to be sufficient for its retrograde transport in non-neuronal cells.[24] However, the exact biophysical parameters such as diffusion coefficients and the velocity of retrogradely transported NF-κB were unknown.

Single-particle tracking (SPT) of fluorophore-labelled receptors in the plasma membrane of a live cell provides valuable information on dynamics and interactions.[25] In combination with photoswitchable fluorophores,[26] SPT allows the observation of a large number of molecules by stochastically activating only a small subset of fluorophores at a given time and tracking them until photobleaching. This cycle of photoactivation, tracking, and photobleaching is repeated many (often a few thousand) times. Profiting from the pool of labelled biomolecules in a sample, a large number of single-molecule trajectories are recorded. SPT with photoactivated-localization

*Address all correspondence to: Darius Widera, E-mail: d.widera@reading.ac.uk; Mike Heilemann, E-mail: heilemann@chemie.uni-frankfurt.de; Christian Kaltschmidt, E-mail: c.kaltschmidt@uni-bielefeld.de

†Equal contributions by Darius Widera and Christin Klenke.

‡Present address: NSF Erdmann Analytics, Rheda-Wiedenbrück, Germany

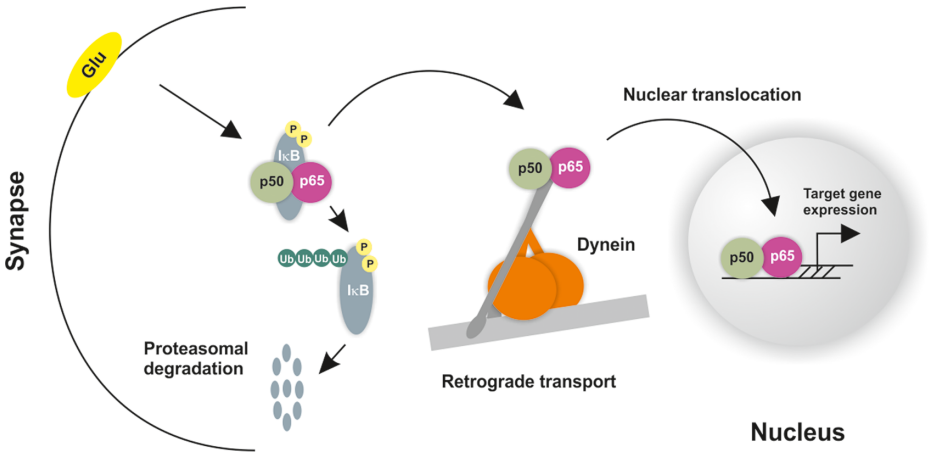

Fig. 1 Synaptic activity promotes dynein-dependent retrograde transport of NF-κB to the nucleus. Schematic presentation of retrograde transport of NF-κB in neurons. After stimulation of the neuron with an activator such as glutamate, upstream kinases induce phosphorylation of the inhibitory protein IκB stimulating its proteasomal degradation. This allows the binding of p65/p50 heterodimers to the dynein/dynactin motor proteins. After the assembly of the complex and its retrograde movement along the microtubule network, NF-κB translocates into the nucleus without disruption of the complex and induces transcription of specific target genes.

microscopy (SPT-PALM[27]) allows longer observation times, provides better statistics,[28,29] and allows high-density mapping of molecular movements.[30]

In order to study the dynamics of retrogradely transported NF-κB in neurons at the single-molecule level, we applied SPT-PALM[27,31] and used the fluorescent protein tandem-Eos-FP (tdEos) as a reporter.[27,28] tdEos is photoconverted from a green-fluorescent to an orange-fluorescent species by irradiation with 405 nm light.[32] Following this procedure, a small stochastic subset of the tdEos is transferred into the active (orange-fluorescent) state and tracked as single molecules. In the present study, we used this technique to visualize p65-tdEos (NF-κB subunit fused to tdEos) with a localization precision of 26 nm [Fig. 2(a)].

We investigated the glutamate-induced transport of NF-κB p65 in living hippocampal neurons with single-molecule resolution and determined the respective diffusion coefficients. Finally, we demonstrated that synaptic activity leads to an increased mobility of retrogradely and anterogradely transported neuronal NF-κB p65.

2 Results and Discussion

Hippocampal neurons transfected with p65-tdEos were identified by widefield imaging detecting the green fluorescence signal from unconverted p65-tdEos. After identification of the soma (containing the nucleus), neurites of transfected cells were irradiated with low intensities of ultraviolet (UV) light and single p65-tdEos molecules were tracked by their orange

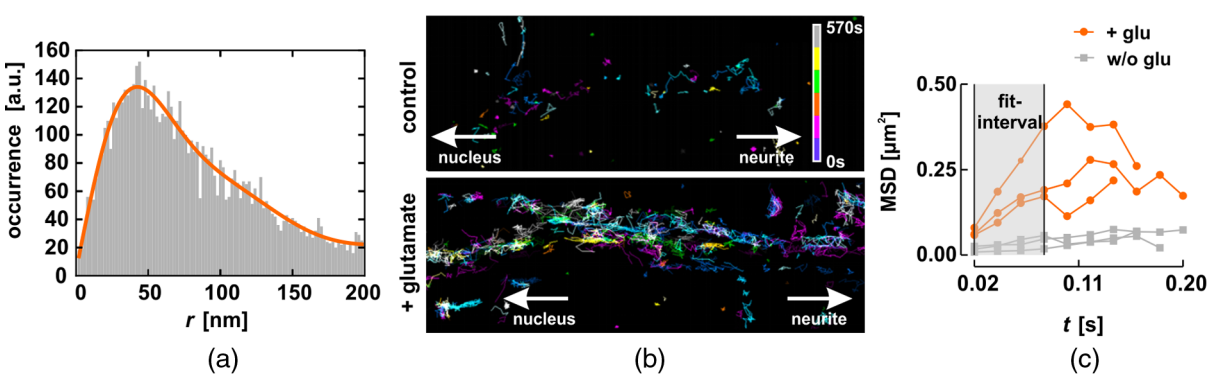

Fig. 2 SPT-PALM imaging of NF-κB p65 in hippocampal neurons. (a) The NF-κB p65 subunit was fused to the photoactivatable fluorescent protein tdEos that can be photoconverted by irradiation with UV light. Transfected neurons were identified in widefield fluorescence mode by detecting the green fluorescence signal of the tdEos in p65-tdEos. A small stochastic subset of the p65-tdEos was photoconverted from a green-fluorescent to an orange-fluorescent species and tracked as single molecules. Localization precision for tdEos was determined to 26 nm using a nearest neighbor approach, as described in Ref. 42. (b) Map of single particle trajectories (middle and lower panel) revealed highly increased mobility of p65-tdEos in neurites after glutamate stimulation compared to controls. Representative data set from a single cell for both conditions is shown. (c) Exemplary MSD plots from single-molecule trajectories of untreated and glutamate-treated p65-tdEos. The first four MSD values were considered for extracting the diffusion coefficient.

fluorescence. Several thousands of trajectories per cell were recorded and used to generate a trajectory map [Fig. 2(b)].

Next, we compared the mobility of NF-κB p65 in unstimulated and glutamate-treated neurons. We observed that glutamate treatment led to an increased mobility of p65-tdEos particles compared to the baseline control [Fig. 2(b)]. This increase in mobility is in general accordance with the reports on rapid retrograde transport of NF-κB in neurons after glutamate treatment.[11,22]

We then calculated the mean diffusion coefficient (D_{mean}) of p65-tdEos molecules from the SPT-PALM data (Fig. 3). In the absence of stimulation (baseline), p65-tdEos molecules showed a D_{mean} of 0.12 ± 0.05 $\mu m^2/s$ [Fig. 3(a)]. Stimulation with glutamate resulted in a higher occurrence of fast molecules (D_{mean} of 0.61 ± 0.03 $\mu m^2/s$) compared to unstimulated controls [Figs. 3(a) and 3(b)] and narrowed the distribution of single-molecule diffusion coefficients [Figs. 3(a) and 3(b)]. Notably, the D_{mean} measured for p65-tdEos without stimulation is in a similar range to the diffusion coefficient reported for the cytoplasmic HIV Gag-Eos fusion (0.11 ± 0.08 $\mu m^2/s$).[27] After stimulation with glutamate, D_{mean} of p65-tdEos is similar to the mobile fraction of membrane residing α-amino-3-hydroxy-5-methyl-4-isoxazolepropionic acid receptors with a diffusion coefficient of >0.5 $\mu m^2/s$.[33] We further followed how the mobility of p65-tdEos developed with time and found that the glutamate-dependent increase in D_{mean} persists for at least 400 s [Fig. 3(d)].

Next, we determined the extent to which glutamate affects the immobile fraction as well as retrogradely and anterogradely transported p65-tdEos particles. In glutamate-stimulated neurons, we recorded a lower occurrence of immobile molecules in neurites that was accompanied by a significant increase in retrogradely transported p65-tdEos [Fig. 4(a)]. Further, although not significant, a slight increase of anterogradely transported molecules was measured. Finally, we determined the velocities of single transported p65-tdEos particles. Although glutamate treatment resulted in heterogeneous velocity distribution for both retrograde and anterograde transport, a significantly increased mean velocity was assessed in both directions [Fig. 4(b)]. Specifically, glutamate treatment resulted in an increase of the mean retrograde velocity from 10.9 ± 1.9 to 15 ± 4.9 $\mu m/s$, whereas a mean velocity increase from 9 ± 1.3 to 14 ± 3 $\mu m/s$ was observed for the anterograde transport. Notably, the mean velocities calculated for p65-tdEos are in the same range reported for the transport of NGF in neurites of rat sympathetic neurons (~3 to 6 $\mu m/s$) as measured in compartmented cultures after applying radioactive ^{125}I-NGF.[34] In neuronal cells, the transport of mitochondria is accomplished

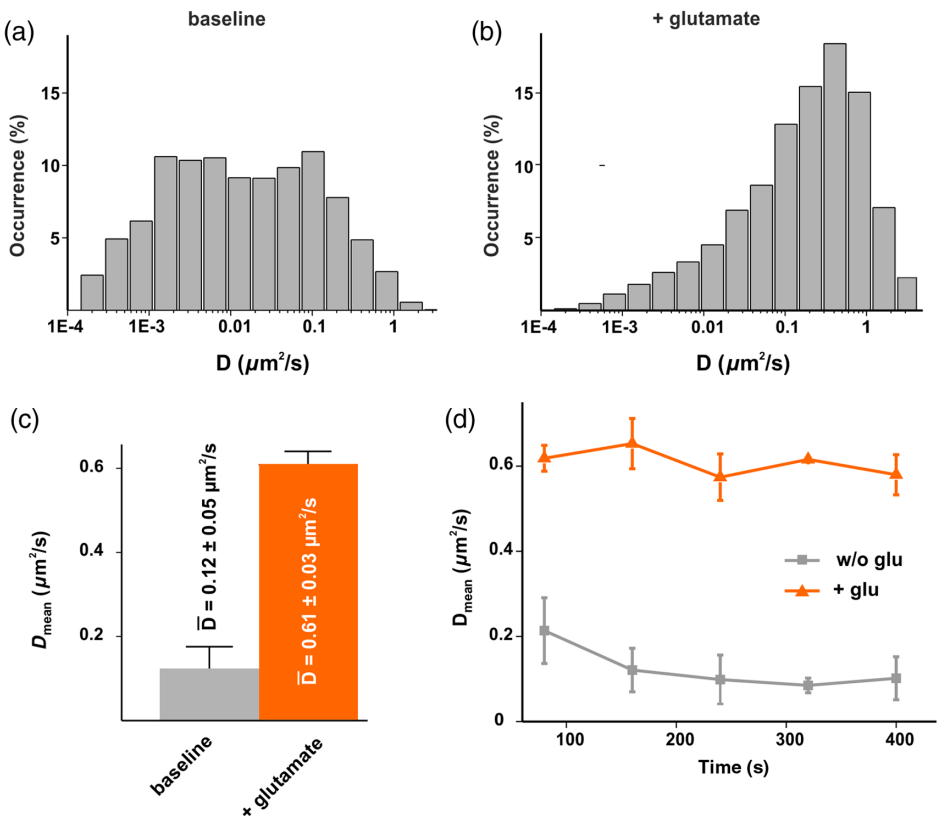

Fig. 3 (a)–(b) Effect of glutamate on the distribution of diffusion coefficients of NF-κB in hippocampal neurons. Note that glutamate treatment narrows the distribution of single-molecule diffusion coefficients compared to the control. (c) Average diffusion coefficient D_{mean} of p65-tdEos under baseline conditions and after treatment with glutamate monitored over time (a representative data set from a single cell each is shown). Glutamate treatment leads to significantly increased D_{mean}. Without stimulation p65 molecules showed D_{mean} of 0.12 ± 0.05 $\mu m^2/s$. Stimulation with glutamate resulted in a strongly increased occurrence of fast particles and D_{mean} of p65 to 0.61 ± 0.03 $\mu m^2/s$. (d) D_{mean} of p65-tdEos under control conditions and after treatment with glutamate monitored over time (a representative data set from a single cell each is shown). Error bars: SEM.

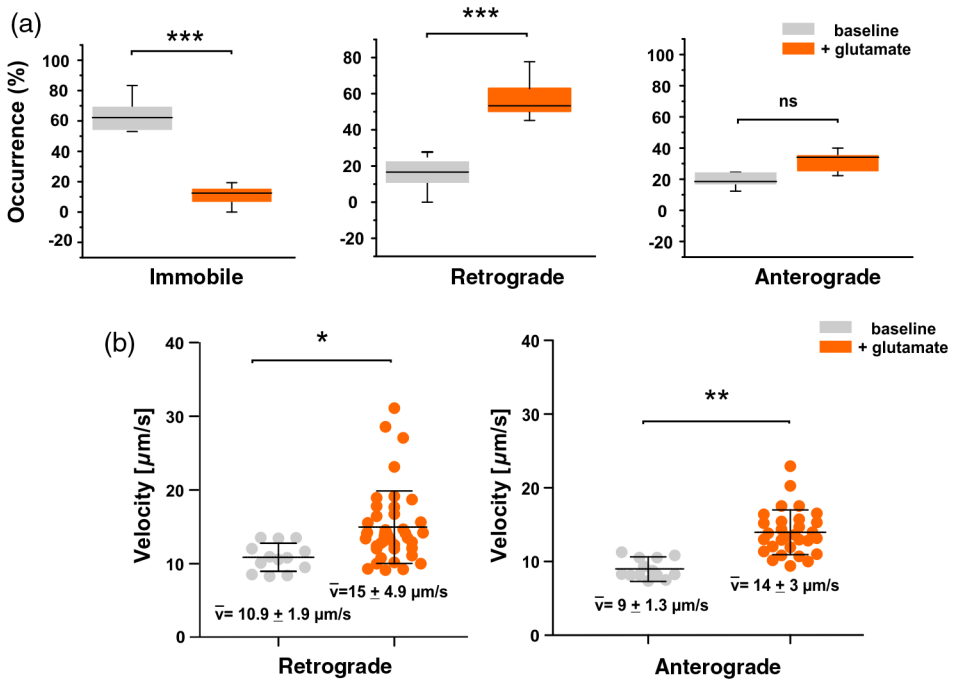

Fig. 4 (a) Effect of glutamate on velocity of retrogradely and anterogradely transported p65-tdEos particles. Single-molecule data were used to calculate the occurrence of immobile and retro- and anterogradely transported p65. Treatment of hippocampal neurons with glutamate resulted in significantly decreased amount of immobile particles and strongly increased retrograde transport. (b) Glutamate treatment increases the mean velocity of retrogradely and anterogradely transported p65-tdEos.

by microtubule-based motors (kinesins and dynein) with velocities ranging from ~5 to 30 μm/s.[35] Moreover, flagellar dyneins achieve a velocity of up to 19 μm/s (reviewed in Refs. 36, 37), which is again in general accordance with the mean velocity of 15 μm/s for p65-tdEos after glutamate treatment (this study).

In summary, we report that glutamate stimulation promotes an increase in mobility of the NF-kB subunit p65 in living hippocampal neurons. Exposure of neurons to glutamate leads to an increased mean diffusion coefficient of p65-tdEos and an increase in the velocity of both retrogradely and anterogradely transported NF-κB p65 in neurites.

3 Methods

3.1 *Astrocyte Cultures*

Mouse astrocytes were prepared from the cortex of postnatal day 1 (P1) BL6 mice, after treatment with 1× Trypsin/EDTA (PAA, Pasching, Austria). The astrocytes were washed with prewarmed DMEM (37°C, PAA) and transferred to DMEM containing 2 mM L-glutamine, 100 U/ml penicillin and streptomycin and 10% fetal bovine serum (PAA). Cells were cultured in a humidified incubator at 95% air and 5% CO_2. One day prior to hippocampi preparation, astrocyte growth was blocked with 10 μg/ml mitomycin (Sigma-Aldrich, Deisenhofen, Germany) for 1.5 h followed by washing with DMEM (PAA) and cultivation in DMEM supplemented with 2 mM L-glutamine, 100 U/ml penicillin and streptomycin, and 10% fetal bovine serum (PAA). Prior to preparation of the hippocampi, the astrocytes were transferred to prewarmed Neurobasal medium (Invitrogen, Darmstadt, Germany) containing B27 supplement (Invitrogen), 2 mM L-glutamine (PAA), 100 U/ml penicillin (PAA), and 100 U/ml streptomycin (PAA).

3.2 *Hippocampal Neuron Cultures*

Primary cultures of mouse hippocampal neurons were prepared from the hippocampi of E18-E19 BL6 mouse embryos, after treatment with 1× Trypsin/ETDA [15 min, 37°C; (0.05%/0.002% in PBS), PAA]. The hippocampi were washed with prewarmed DMEM (37°C) containing 10% FCS, to stop trypsin activity and transferred to prewarmed DMEM (PAA) supplemented with 2 mM L-glutamine, 100 U/ml penicillin (PAA), 100 U/ml streptomycin (PAA), and 10% foetal bovine serum (PAA). The cells were dissociated under these conditions using a fire-polished Pasteur pipette followed by seeding on poly-D-Lysine (Sigma-Aldrich) coated coverslips at a density of 50,000 cells/18 mm. The cultures were maintained in a humidified incubator at 5% CO_2 for 60 min to allow adherence. Subsequently, neurons on coverslips were placed on top astrocyte cultures and further cultivated at 5% CO_2.

3.3 *Anesthesia of Neuronal Activity for Baseline of Nuclear NF-κB and Glutamate Treatment*

Twenty four hours prior to experimentation, hippocampal neuron cultures were treated with 40 μM 6-cyano-7-nitroquinoxaline-2,3-dione (Sigma-Aldrich), 100 μM 2-amino-5-phosphonopentanoic acid (Sigma-Aldrich), and 10 μM nimodipine (Sigma-Aldrich) to establish a stable and low baseline of nuclear NF-κB as described before.[22,23] Afterward, neurons were washed and exposed to 300 μM glutamate or PBS (Sigma-Aldrich) for 5 min in the absence of the inhibitors at 37°C. Subsequently,

the stimulus was washed out and cultures were incubated with complete medium at 37°C for 90 min.

3.4 *Single-Particle Tracking with Photoactivated-Localization Microscopy Imaging, Single Molecule Segmentation and Tracking*

The tdEos fusion to p65 was achieved by subcloning of p65[38] into pcDNA3-Flag1-td-EosFP (MoBiTec). Hippocampal neurons were transiently transfected with p65-tdEos overnight using Effectene (Qiagen) according to the manufacturer's guidelines. Cells were imaged at 37°C in an open chamber (Ludin Chamber, Life Imaging Services) mounted on an inverted motorized microscope (Nikon Ti-E, Nikon, Japan) equipped with a 100× 1.45NA PL-APO (Nikon) objective and a perfect focus system. To identify transfected cells, the fluorescence from the nonphotoconverted tdEos was recorded using excitation light at 488 nm and a GFP filter cube (ET470/40, T495LPXR, and ET525/50, Chroma). Cells expressing the tdEos constructs were selected for SPT-PALM imaging. Irradiation at 405 nm using a diode laser (Omicron) at low intensities leads to photoconversion of tdEos which was read-out with a 561-nm laser (Cobolt, Sweden). The respective irradiation intensities were adjusted to keep the number of the stochastically activated molecules at low single molecule density, and leave single molecules fluorescent during multiple frames before bleaching. The fluorescence was collected by the combination of a dichroic and emission filters (D101-R561 and F39-617, respectively, Chroma) and a sensitive EMCCD camera (Evolve, Photometric). The acquisition was steered by Metamorph software (Molecular Devices) in streaming mode at 50 frames/s (20 ms exposure time). Recording times for single cells varied from 5 to 30 min. Single molecule fluorescent spots were localized in each image frame and tracked over time using a combination of wavelet segmentation and simulated annealing algorithms.[39–41] The localization accuracy of the SPT-PALM microscope under our experimental conditions was quantified using fixed samples expressing tdEos. Localization precision was determined to 26 nm using a nearest neighbor approach, according to Ref. 42. The software package used to visualize and derive quantitative data on protein localization and dynamics was custom written for Metamorph (Visitron Systems GmbH, Puchheim, Germany).

An average of >500 trajectories per cell with a minimum trajectory length of eight frames was obtained and analyzed. For these trajectories, the mean square displacement (MSD) was calculated according to the equation $\mathrm{MSD} = \Delta x^2 + \Delta y^2$. The diffusion coefficient was extracted by approximating the first four points of a plot of D_{mean} versus time using the relationship of $\mathrm{MSD} = 4\mathrm{Dt}$. The mean diffusion coefficient (D_{mean}) was calculated as an average from all single-molecule diffusions. Kymographs were used to define immobile, retrogradely, and anterogradely moving particles (according to the position of the soma and the neurites). For exemplary MSD-analysis see Fig. 2(c).

3.5 *Statistical Analysis*

Statistical significance was determined by ANOVA using the Bonferroni post-test, or if appropriate using two-tailed Student's *t*-tests using GraphPad's Prim Software. p values <0.05 were considered significant.

Acknowledgments

This study was supported by the grant of the German Research Foundation (DFG) to CK. MeH, MiH, and SM were supported by the Systems Biology Initiative (FORSYS, Grant No. 0135262) of the German Ministry of Research and Education (BMBF) and the German Research Foundation (SFB 902). DN was supported by a Marie-Curie Intra European Fellowship. The authors declare that they have no competing financial interests. We thank Dr. Graeme Cottrell for critical reading.

References

1. M. P. Mattson et al., "Roles of nuclear factor kappaB in neuronal survival and plasticity," *J. Neurochem.* **74**(2), 443–456 (2000).
2. V. Fridmacher et al., "Forebrain-specific neuronal inhibition of nuclear factor-kappaB activity leads to loss of neuroprotection," *J. Neurosci.* **23**(28), 9403–9408 (2003).
3. M. K. Meffert et al., "NF-kappa B functions in synaptic signaling and behavior," *Nat. Neurosci.* **6**(10), 1072–1078 (2003).
4. B. Kaltschmidt, D. Widera, and C. Kaltschmidt, "Signaling via NF-kappaB in the nervous system," *Biochim. Biophys. Acta* **1745**(3), 287–299 (2005).
5. M. K. Meffert and D. Baltimore, "Physiological functions for brain NF-kappaB," *Trends Neurosci.* **28**(1), 37–43 (2005).
6. M. P. Mattson and M. K. Meffert, "Roles for NF-kappaB in nerve cell survival, plasticity, and disease," *Cell Death Differ.* **13**(5), 852–860 (2006).
7. B. Kaltschmidt and C. Kaltschmidt, "NF-kappaB in the nervous system," *Cold Spring Harbor Perspect. Biol.* **1**(3), a001271 (2009).
8. C. Kaltschmidt, B. Kaltschmidt, and P. A. Baeuerle, "Brain synapses contain inducible forms of the transcription factor NF-kappa B," *Mech. Dev.* **43**(2–3), 135–147 (1993).
9. C. Kaltschmidt et al., "Constitutive NF-kappa B activity in neurons," *Mol. Cell. Biol.* **14**(6), 3981–3992 (1994).
10. C. Kaltschmidt, B. Kaltschmidt, and P. A. Baeuerle, "Stimulation of ionotropic glutamate receptors activates transcription factor NF-kappa B in primary neurons," *Proc. Natl. Acad. Sci. U. S. A.* **92**(21), 9618–9622 (1995).
11. H. Wellmann, B. Kaltschmidt, and C. Kaltschmidt, "Retrograde transport of transcription factor NF-kappa B in living neurons," *J. Biol. Chem.* **276**(15), 11821–11829 (2001).
12. T. Suzuki et al., "Presence of NF-kB-like and IkB-like immunoreactivities in postsynaptic densities," *NeuroReport* **8**(13), 2931–2935 (1997).
13. P. J. Meberg et al., "Gene expression of the transcription factor NF-kB in hippocampus: regulation by synaptic activity," *Mol. Brain Res.* **38**(2), 179–190 (1996).
14. A. Salles, A. Romano, and R. Freudenthal, "Synaptic NF-kappa B pathway in neuronal plasticity and memory," *J. Physiol. Paris* **108**(4–6), 256–262 (2014).
15. B. Kaltschmidt and C. Kaltschmidt, "NF-KappaB in long-term memory and structural plasticity in the adult mammalian brain," *Front. Mol. Neurosci.* **8**, 69 (2015).
16. C. L. Howe, "Modeling the signaling endosome hypothesis: why a drive to the nucleus is better than a (random) walk," *Theor. Biol. Med. Model.* **2**, 43 (2005).
17. T. H. Ch'ng and K. C. Martin, "Synapse-to-nucleus signaling," *Curr. Opin. Neurobiol.* **21**(2), 345–352 (2010).
18. S. Hanz and M. Fainzilber, "Integration of retrograde axonal and nuclear transport mechanisms in neurons: implications for therapeutics," *Neuroscientist* **10**(5), 404–408 (2004).
19. R. B. Vallee et al., "Dynein: an ancient motor protein involved in multiple modes of transport," *J. Neurobiol.* **58**(2), 189–200 (2004).
20. S. Maday et al., "Axonal transport: cargo-specific mechanisms of motility and regulation," *Neuron* **84**(2), 292–309 (2014).
21. S. Millecamps and J. P. Julien, "Axonal transport deficits and neurodegenerative diseases," *Nat. Rev. Neurosci.* **14**(3), 161–176 (2013).
22. I. Mikenberg et al., "Transcription factor NF-kappaB is transported to the nucleus via cytoplasmic dynein/dynactin motor complex in hippocampal neurons," *PLoS One* **2**(7), e589 (2007).
23. C. K. Shrum, D. Defrancisco, and M. K. Meffert, "Stimulated nuclear translocation of NF-kappaB and shuttling differentially depend on

dynein and the dynactin complex," *Proc. Natl. Acad. Sci. U. S. A.* **106**(8), 2647–2652 (2009).
24. I. Mikenberg et al., "TNF-alpha mediated transport of NF-kappaB to the nucleus is independent of the cytoskeleton-based transport system in non-neuronal cells," *Eur. J. Cell Biol.* **85**(6), 529–536 (2006).
25. G. J. Schutz, H. Schindler, and T. Schmidt, "Single-molecule microscopy on model membranes reveals anomalous diffusion," *Biophys. J.* **73**(2), 1073–1080 (1997).
26. A. Furstenberg and M. Heilemann, "Single-molecule localization microscopy-near-molecular spatial resolution in light microscopy with photoswitchable fluorophores," *Phys. Chem. Chem. Phys.* **15**(36), 14919–14930 (2013).
27. S. Manley et al., "High-density mapping of single-molecule trajectories with photoactivated localization microscopy," *Nat. Methods* **5**(2), 155–157 (2008).
28. M. Heidbreder et al., "TNF-alpha influences the lateral dynamics of TNF receptor I in living cells," *Biochim. Biophys. Acta* **1823**(10), 1984–1989 (2012).
29. P. J. Zessin, A. Sporbert, and M. Heilemann, "PCNA appears in two populations of slow and fast diffusion with a constant ratio throughout S-phase in replicating mammalian cells," *Sci. Rep.* **6**, 18779 (2016).
30. D. Nair et al., "Super-resolution imaging reveals that AMPA receptors inside synapses are dynamically organized in nanodomains regulated by PSD95," *J. Neurosci.* **33**(32), 13204–13224 (2013).
31. J. B. Sibarita, "High-density single-particle tracking: quantifying molecule organization and dynamics at the nanoscale," *Histochem. Cell Biol.* **141**(6), 587–595 (2014).
32. J. Wiedenmann et al., "EosFP, a fluorescent marker protein with UV-inducible green-to-red fluorescence conversion," *Proc. Natl. Acad. Sci. U. S. A.* **101**(45), 15905–15910 (2004).
33. P. Opazo et al., "CaMKII triggers the diffusional trapping of surface AMPARs through phosphorylation of stargazin," *Neuron* **67**(2), 239–252 (2010).
34. D. R. Ure and R. B. Campenot, "Retrograde transport and steady-state distribution of 125I-nerve growth factor in rat sympathetic neurons in compartmented cultures," *J. Neurosci.* **17**(4), 1282–1290 (1997).
35. W. Song et al., "Mutant huntingtin binds the mitochondrial fission GTPase dynamin-related protein-1 and increases its enzymatic activity," *Nat. Med.* **17**(3), 377–382 (2011).
36. D. D. Ginty and R. A. Segal, "Retrograde neurotrophin signaling: Trking along the axon," *Curr. Opin. Neurobiol.* **12**(3), 268–274 (2002).
37. R. B. Campenot and B. L. MacInnis, "Retrograde transport of neurotrophins: fact and function," *J. Neurobiol.* **58**(2), 217–229 (2004).
38. C. Klenke et al., "Hsc70 is a novel interactor of NF-kappaB p65 in living hippocampal neurons," *PLoS One* **8**(6), e65280 (2013).
39. I. Izeddin et al., "Wavelet analysis for single molecule localization microscopy," *Opt. Express* **20**(3), 2081–2095 (2012).
40. V. Racine et al., "Visualization and quantification of vesicle trafficking on a three-dimensional cytoskeleton network in living cells," *J. Microsc.* **225**(Pt 3), 214–228 (2007).
41. V. Racine et al., "Multiple-target tracking of 3-D fluorescent objects based on simulated annealing," in *3rd IEEE Int. Symp. on Biomedical Imaging: Nano to Macro, 2006*, pp. 1020–1023 (2006).
42. U. Endesfelder et al., "A simple method to estimate the average localization precision of a single-molecule localization microscopy experiment," *Histochem. Cell Biol.* **141**(6), 629–638 (2014).

Biographies for the authors are not available.